Supplementary information

Lis1 regulates asymmetric division in hematopoietic stem cells and in leukemia

Bryan Zimdahl[1,2,3]§, Takahiro Ito[1,2]§, Allen Blevins[1,2], Jeevisha Bajaj[1,2], Takaaki Konuma[1,2], Joi Weeks[1,2], Claire S. Koechlein[1,2], Hyog Young Kwon[1,2], Omead Arami[1,2], David Rizzieri[4], H. Elizabeth Broome[5,6], Charles Chuah[7,8], Vivian G. Oehler[9], Roman Sasik[10], Gary Hardiman[10] and Tannishtha Reya[1,2,3,6]*

§These authors contributed equally to this work

[1]Department of Pharmacology, University of California San Diego School of Medicine, La Jolla 92093

[2] Sanford Consortium for Regenerative Medicine, La Jolla, CA, 92093

[3]Department of Pharmacology and Cancer Biology, Duke University Medical Center, Durham, NC, 27710

[4]Division of Cell Therapy, Department of Medicine, Duke University Medical Center, Durham, NC, 27710

[5]Department of Pathology, University of California San Diego School of Medicine, La Jolla, CA, 92093

[6]Moores Cancer Center, University of California San Diego School of Medicine, La Jolla, CA, 92093

[7]Department of Haematology, Singapore General Hospital, Singapore

[8]Cancer and Stem Cell Biology Program, Duke-NUS Graduate Medical School, Singapore

[9]Clinical Research Division, Fred Hutchinson Cancer Research Center, Seattle, WA, 98109

[10]Department of Medicine, University of California San Diego School of Medicine, La Jolla, 92093

*Correspondence should be addressed to T.R. (treya@ucsd.edu)

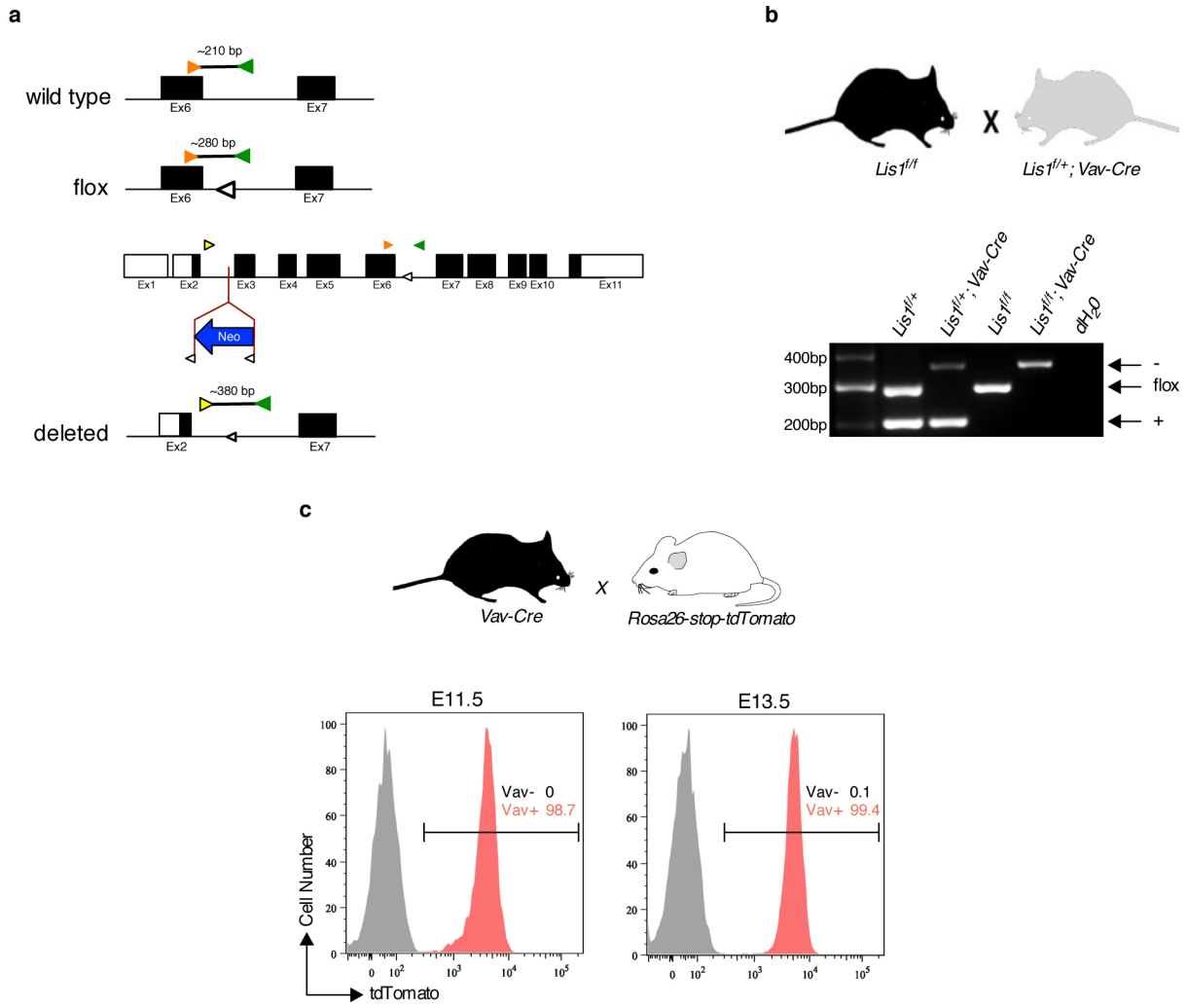

Supplementary Figure 1. Efficiency of *Vav-Cre*-mediated recombination in fetal HSCs.
(a) The position of three primers (colored triangles) used to detect the wild type, floxed and deleted *Lis1* alleles are shown. LoxP sites are indicated by open triangles. Neo, neomycin resistance gene. **(b)** The schematic indicates the strategy for deletion of *Lis1* in hematopoietic cells using mice homozygous for the floxed *Lis1* allele crossed to mice heterozygous for the floxed *Lis1* allele and carrying a transgene in which expression of the Cre recombinase is driven by the *Vav* promoter (top). Analysis of deletion efficiency by genomic PCR within $CD45^+$ PI^- (Propidium iodide) fetal liver cells from E14.5 littermates (bottom). **(c)** *Vav-Cre*-mediated recombination in fetal HSCs (c-Kit^+ Lin^- $AA4.1^+$; KL $AA4.1^+$). *Vav-Cre* mice were crossed to *Rosa26-stop-tdTomato* reporter mice. Representative FACS histogram shows reporter activity (Tomato expression) which is reflective of *Lis1* deletion efficiency in KL $AA4.1^+$ cells from control (*Tomato+; Vav-Cre-*) and *Tomato+; Vav-Cre+* littermates at E11.5 and E13.5; *n*=2-7 mice for each genotype for each gestational age.

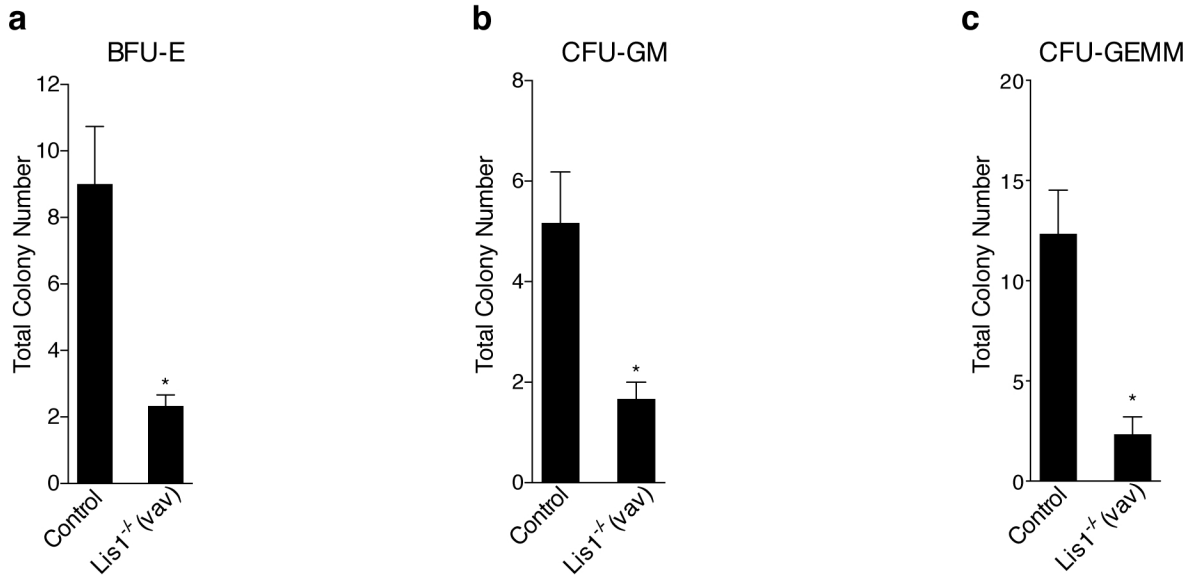

Supplementary Figure 2. CFU-C assays from fetal livers.

(a-c) CFU-C assays from E12.5 fetal livers. Data in Figure 1d showing the total number of colonies generated from plating 5000 whole fetal liver cells from Control (*Lis1*$^{f/+}$ *or Lis1*$^{f/f}$) and *Lis1*$^{-/-}$ (*Lis1*$^{f/f}$*; Vav-Cre*) mice at E12.5 is deconstructed into the number of individual types of colonies generated: BFU-E **(a)**, CFU-GM **(b)** and CFU-GEMM **(c)**. Cells are isolated from 3-6 embryos of each genotype. BFU-E was determined on Day 7 and CFU-GM and CFU-GEMM were determined on Day 10 (n=3 technical replicates, *P=0.0194 for BFU-E, *P=0.0305 for CFU-GM, *P=0.0132 for CFU-GEMM). Error bars show the standard error of mean (SEM).

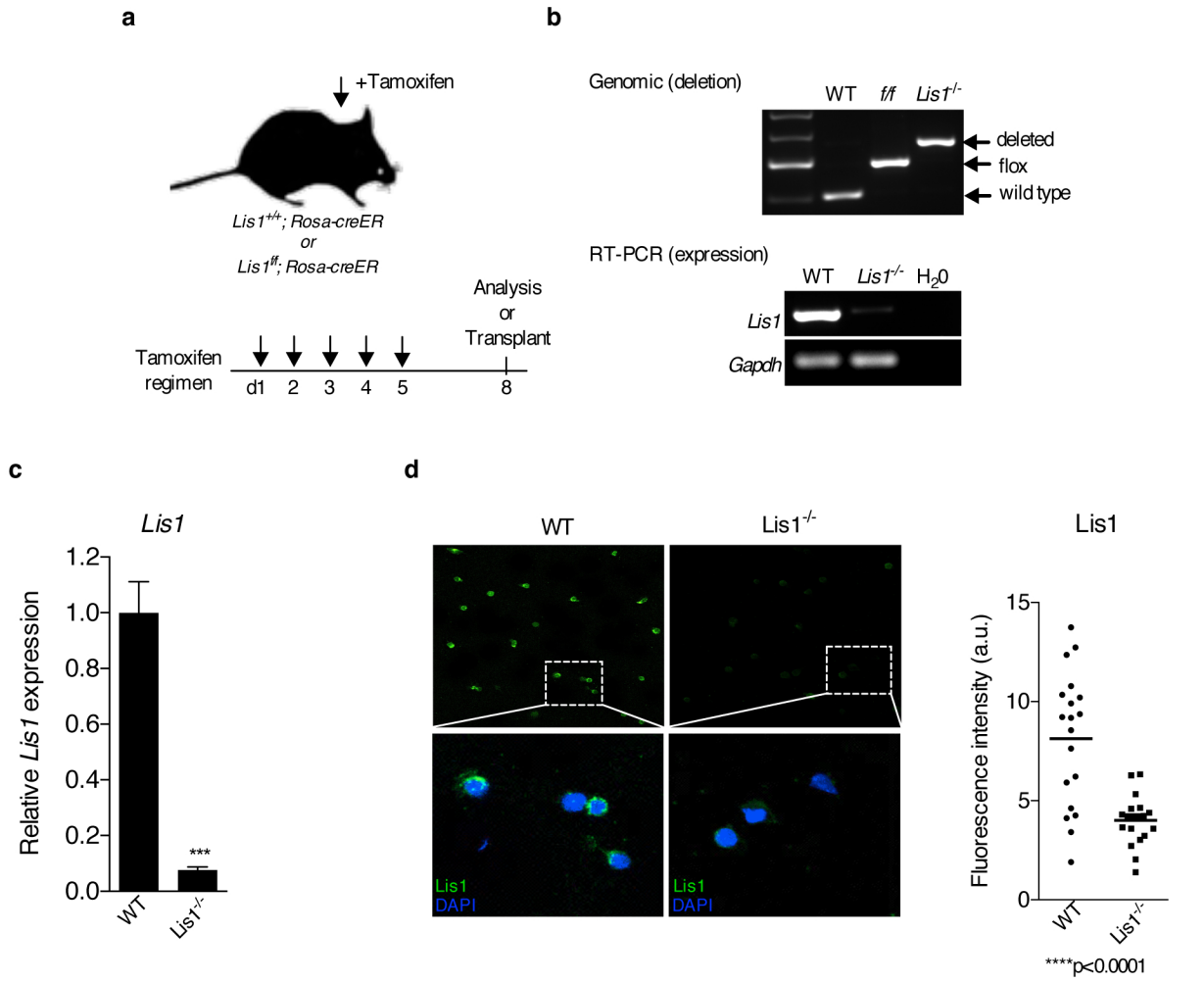

Supplementary Figure 3. *Lis1* deletion in adult HSCs.
(a) Strategy for deletion of *Lis1* in adult mice. Control (*Lis1*$^{+/+}$*; Rosa26-creER/Rosa26-creER*, indicated as *Lis1*$^{+/+}$*; Rosa-creER*) and *Lis1*$^{f/f}$*; Rosa26-creER/Rosa26-creER* (indicated as *Lis1*$^{f/f}$*; Rosa-creER*) mice were administered tamoxifen daily for 5 days. Analyses and cell sorting were performed 3 days post-tamoxifen. **(b)** Analysis of deletion efficiency in HSC-enriched cells by genomic PCR (top) and RT-PCR (bottom). Cells were isolated from tamoxifen-treated control (*Lis1*$^{+/+}$*; Rosa-creER*, indicated as WT), corn oil-treated control (*Lis1*$^{f/f}$*; Rosa-creER*, indicated as *f/f*) and tamoxifen-treated *Lis1*$^{f/f}$*; Rosa-creER* (indicated as *Lis1*$^{-/-}$) mice. **(c)** Analysis of deletion efficiency in HSC-enriched cells by realtime PCR analysis; n=2 independent experiments (technical replicates for each n); ***P=0.0004. Expression levels were normalized and displayed relative to the control TATA-binding protein. All error bars show the standard error of the mean (SEM). **(d)** HSCs (KLS CD48$^-$) isolated from control (WT) and *Lis1*$^{f/f}$*; Rosa-creER* (*Lis1*$^{-/-}$) mice 3 days post-tamoxifen treatment were immunostained with anti-Lis1 antibody (green) and 4′, 6-diamidino-2-phenylindole (DAPI, blue) and fluorescence intensity was quantified; n=19 cells for each genotype, ****P<0.0001. a.u., arbitrary units.

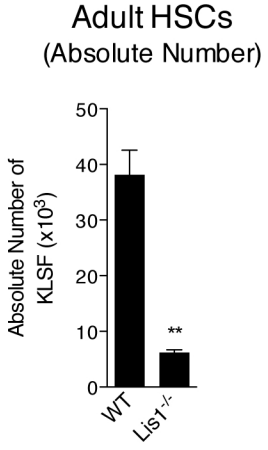

Supplementary Figure 4. Reduction in the absolute number of HSCs in adult *Lis1*$^{-/-}$ mice. Absolute number of adult HSCs (KLSF) from control (WT) and *Lis1*$^{-/-}$ mice; n=4 for WT, n=2 for *Lis1*$^{-/-}$; **P=0.0085.

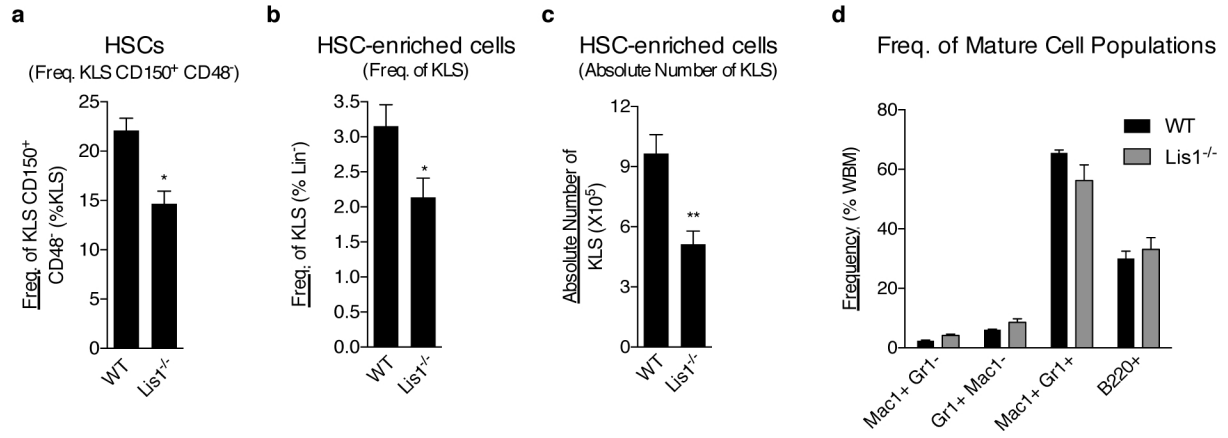

Supplementary Figure 5. Reduction of HSCs precedes defects in differentiated cells.
(a) Average frequency of HSCs (KLS CD150^{+} CD48^{-}) within the HSC-enriched (KLS) population from control (WT) and *Lis1*$^{-/-}$ mice. Mice were administered tamoxifen daily for 3 days. Bone marrow analysis was performed on day 3; *n*=3 for WT, *n*=4 for *Lis1*$^{-/-}$; **P*=0.0103. (**b-d**) Average frequency **(b),** and absolute number **(c)** of KLS cells and average frequencies of mature cell populations **(d)** from control (WT) and *Lis1*$^{-/-}$ mice 1 day post-tamoxifen (daily for 5 days); *n*=6-9 for each genotype; **P*=0.0252 for frequency ***P*=0.0012 for absolute numbers of KLS.

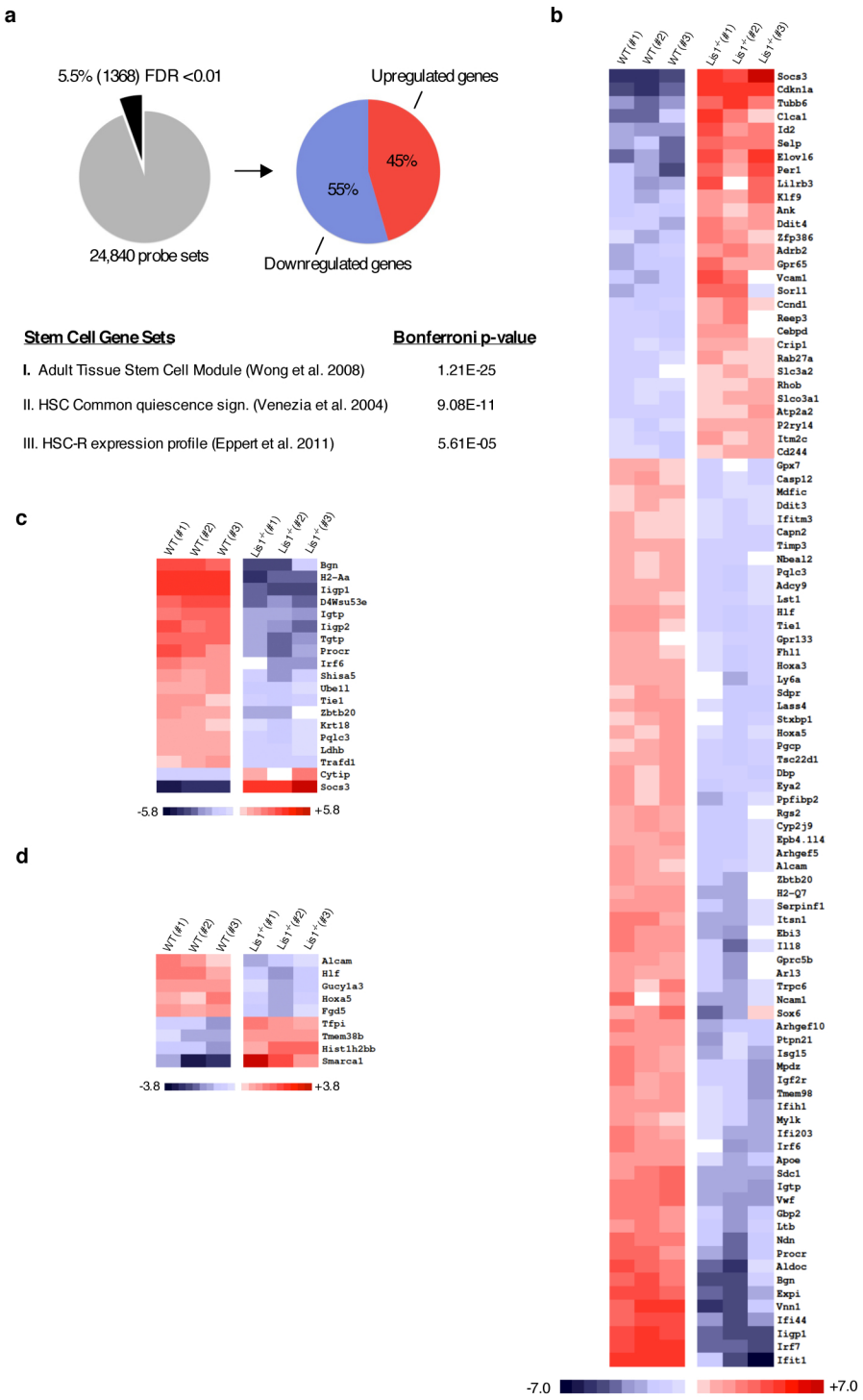

Supplementary Figure 6. Genome wide expression analysis of *Lis1*-deficient HSC-enriched cells.

(a) Comparative gene set enrichment analysis identified 5.5% of genes as changed with a false discovery rate of <0.01; 746 probe sets were down-regulated and 622 probe sets were up-regulated. **(b-d)** Significant differential expression of mRNAs identified previously as part of a stem cell-associated gene signature. Heat map showing expression changes in mRNAs highly enriched in **(b)** Adult Tissue Stem Cell Module (FDR <0.01)[1], Bonferroni *P*-value=1.25E-25; **(c)** HSC-Common quiescence signature[2], Bonferroni *P*-value=9.08E-11; **(d)** HSC-R expression profile[3], Bonferroni *P*-value=5.61E-05 in the *Lis1*-deficient HSC-enriched cells.

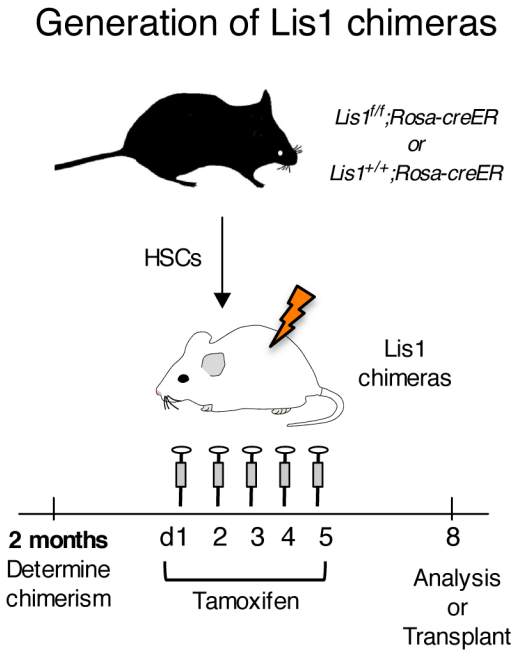

Supplementary Figure 7. Generation of chimeric mice with hematopoietic-specific *Lis1* deletion.

(a) Experimental scheme to generate chimeras with hematopoietic-specific *Lis1* deletion. 1,000 HSCs (KLS CD150$^+$ CD48$^-$) from control (*Lis1*$^{+/+}$*; Rosa-creER*) or *Lis1*$^{f/f}$*; Rosa-creER* (CD45.2$^+$) mice were transplanted into CD45.1$^+$ recipient mice. Two months post-transplantation, an average of ~80% donor-derived chimerism was observed. All recipient mice were administered tamoxifen daily for 5 days and analyses and cell sorting were performed 3 days post-tamoxifen treatment.

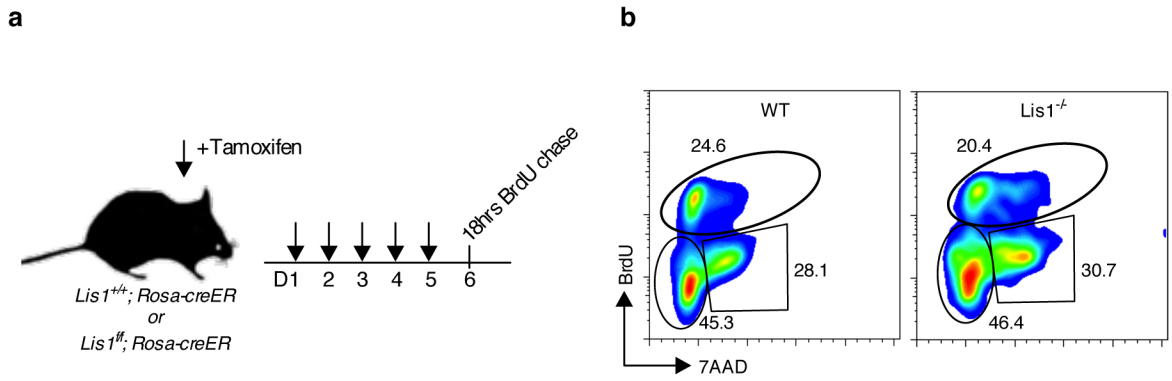

Supplementary Figure 8. Analysis of cell cycle distribution of HSC-enriched cells.
(a) Schematic illustrates the strategy used to determine cell cycle status of hematopoietic cells following *Lis1* deletion. Control (*Lis1*$^{+/+}$*; Rosa-creER*) and *Lis1*$^{f/f}$*; Rosa-creER* mice were administered tamoxifen daily for 5 days (D1-D5). Mice were pulsed with 5-bromodeoxyuridine (BrdU) at 1 day post-injection (D6). After an 18 hr chase period, bone marrow cells were analyzed. (**b**) Representative BrdU/7AAD plot showing cell cycle distribution of KLS (c-Kit^{+} Lin^{-} Sca1^{+}) cells in control (WT) or *Lis1*$^{-/-}$ mice.

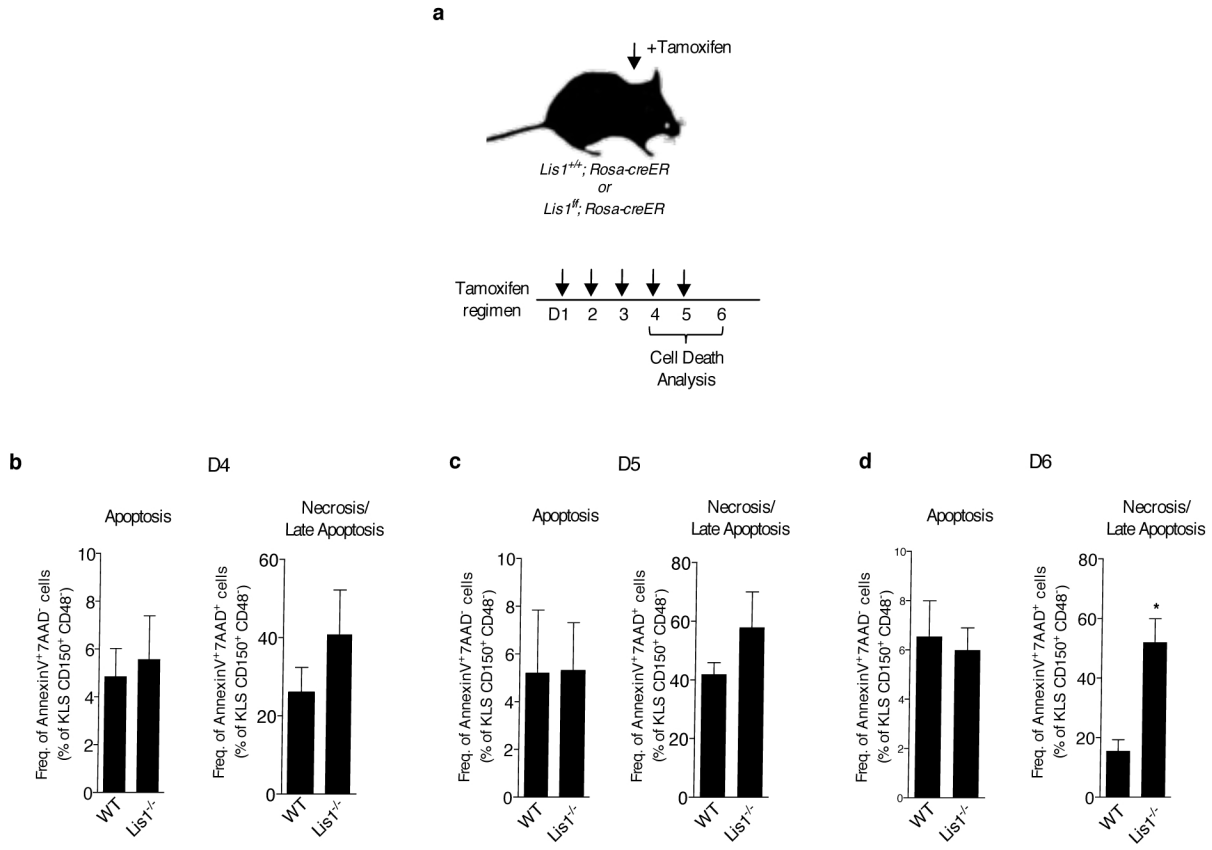

Supplementary Figure 9. Analysis of adult HSC cell death.

(a) Schematic illustrates the strategy used to analyze cell death of hematopoietic cells following *Lis1* deletion. Control (*Lis1*$^{+/+}$*; Rosa-creER*) and *Lis1*$^{f/f}$*; Rosa-creER* mice were administered tamoxifen daily for 5 days (D1-D5). Cell death analysis was performed on D4 and D5 (during tamoxifen treatment) and 1 day post-tamoxifen injections (D6). (**b-d**) Percentage of HSCs (c-Kit^{+} Lin^{-} Sca1^{+} CD150^{+} CD48^{-}) undergoing apoptosis (AnnexinV+ 7AAD-) or undergoing necrosis/late apoptosis (AnnexinV+ 7AAD+) in control (WT) and *Lis1*$^{-/-}$ mice on D4 **(b)**, D5 **(c)** and D6 **(d)**. Data shown are from two independent experiments (n=2-3 per cohort for each day analyzed; *P=0.0141). Data shown in (d) is also shown in Figure 3d. All error bars show the standard error of the mean (SEM).

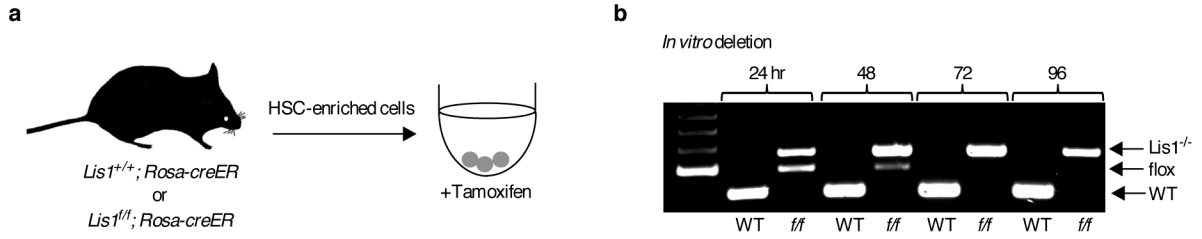

Supplementary Figure 10. Approach and efficiency of *Lis1* deletion *in vitro*.
(a) Schematic illustrates the approach used to delete *Lis1 in vitro*. Briefly, an HSC-enriched fraction of bone marrow cells (cKit$^+$ Lin$^-$ Sca1$^+$; KLS) was isolated from control (*Lis1$^{+/+}$; Rosa-creER*; WT) and *Lis1$^{f/f}$; Rosa-creER* (*f/f*) mice and treated with 4-OH-tamoxifen in liquid media. **(b)** Analysis of deletion efficiency by genomic PCR analysis. Genomic DNA from cultured KLS cells at different time points after 4-OH-tamoxifen treatment. Detailed information regarding primers used is shown in Supplementary Figure 1.

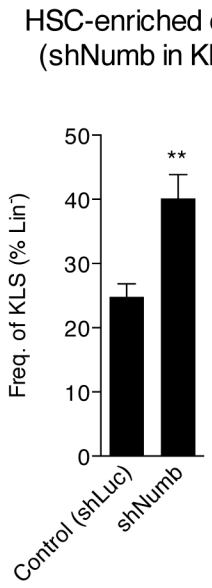

Supplementary Figure 11. shRNA-mediated knockdown of Numb leads to an increase in the frequency of HSC-enriched cells. KLS cells were infected with either control (shLuc) or an shRNA against Numb (shNumb). Average frequency of KLS cells within the infected (GFP^+), Lineage-negative (Lin^-) population at 72 hrs post-infection. Data shown are from two independent experiments. $^{**}P$=0.0048.

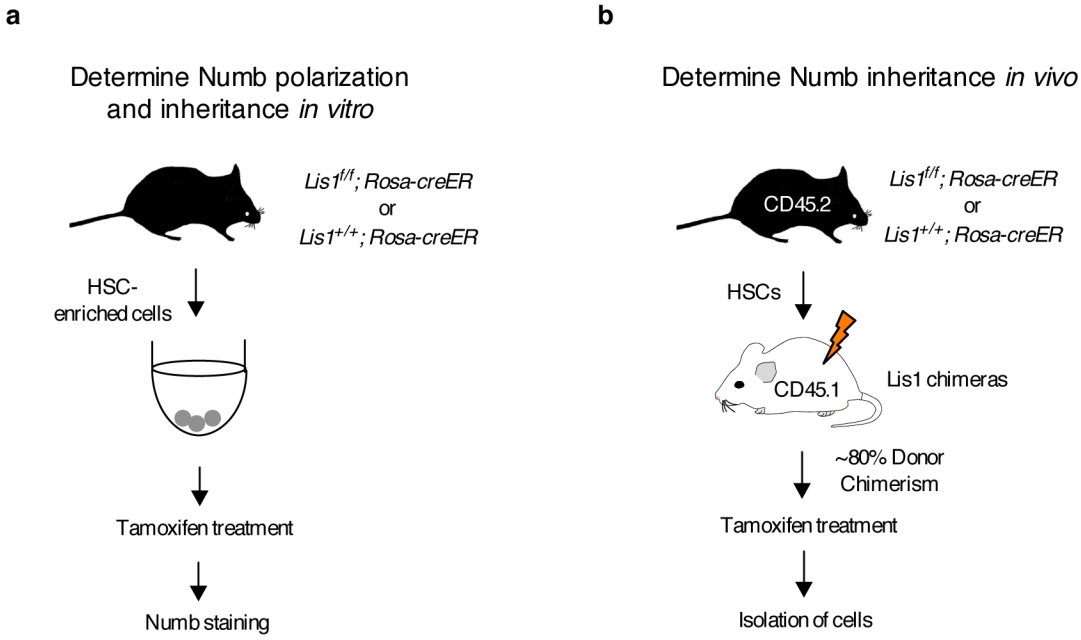

Supplementary Figure 12. Experimental schemes used to determine Numb polarization and inheritance.

(a) Experimental scheme used to determine Numb polarization and inheritance in HSC-enriched cells *in vitro*. KLS cells were isolated from control (*Lis1*$^{+/+}$*; Rosa-creER*) and *Lis1*$^{f/f}$*; Rosa-creER* mice, treated with 4OH-tamoxifen *in vitro* and analyzed 24 hours post-deletion. **(b)** Experimental scheme used to determine Numb inheritance *in vivo*. 1,000 HSCs (KLS CD48^{-} CD150^{+}) from untreated control (*Lis1*$^{+/+}$*; Rosa-creER*) and *Lis1*$^{f/f}$*; Rosa-creER* mice were transplanted into wild type recipients to generate chimeric mice with a wild type microenvironment. Following reconstitution, recipients were treated with tamoxifen and donor-derived lineage negative (Lin^{-}) cells were sorted, fixed and stained to determine Numb inheritance in cells undergoing telophase/cytokinesis.

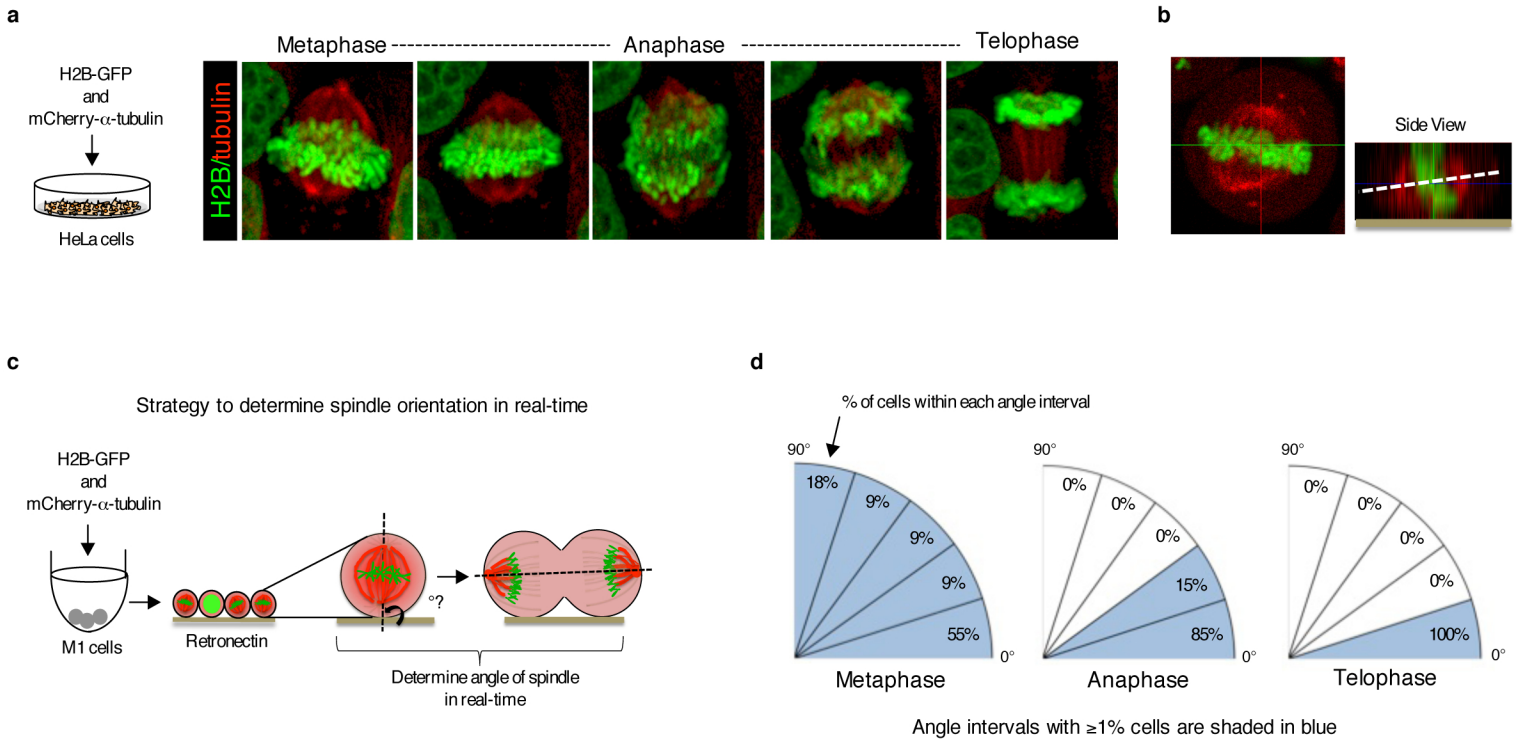

Supplementary Figure 13. Establishment of imaging strategy to track cell division and spindle orientation in real-time.
(a) Schematic illustrates the strategy used to visualize a cell in progressive phases of mitosis in real-time. HeLa cells were retrovirally co-infected with H2B-GFP and mCherry-α-tubulin fusion constructs and individual cells tracked during division (corresponding movie shown in Supplementary Video 1). **(b)** Representative top view (left) and orthogonal view (right) of a GFP^+ $mCherry^+$ HeLa cell in metaphase. The spindle angle relative to the substrate can be measured by drawing a dotted line that bisects the cell's centrosomes. **(c)** Experimental scheme used to determine the orientation of the mitotic spindle in M1 cells. M1 cells were co-infected with H2B-GFP and mCherry-α-tubulin fusion constructs and plated on retronectin-coated slides and their spindle angle relative to the retronectin base was measured over time (corresponding movie shown in Supplementary Video 1). **(d)** Quantification of spindle orientation in M1 cells relative to the retronectin base. Values are expressed as a percentage of M1 cells within each angle interval. Angle intervals in which >1% cells are present are shaded in blue. Data are shown from three independent experiments; *n*=11-15 tracked cells.

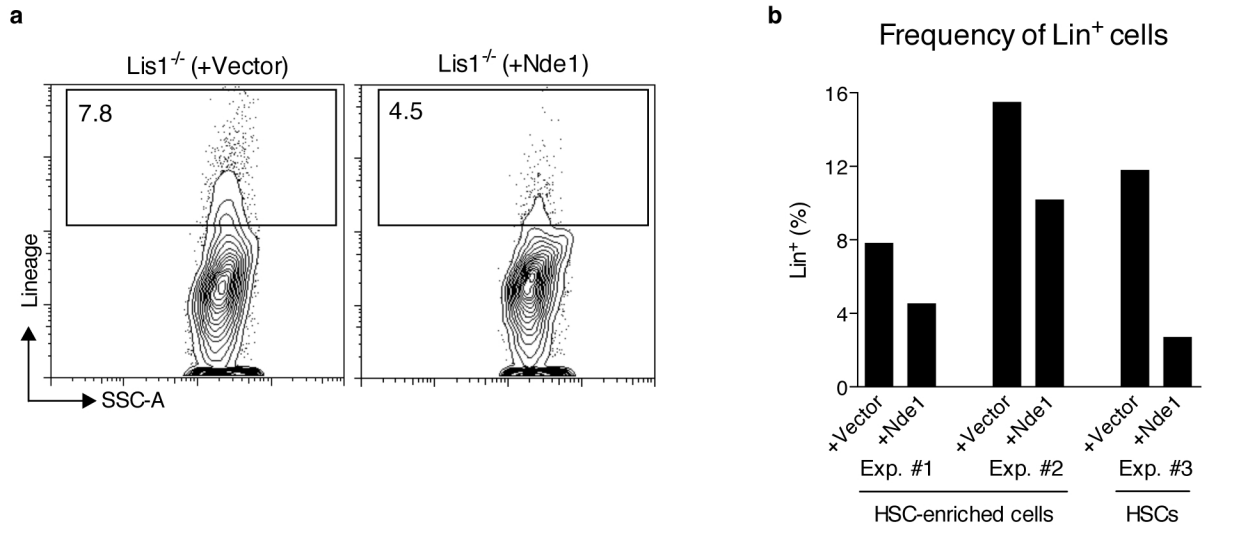

Supplementary Figure 14. Rescue of Lis1 null accelerated differentiation defect by ectopic expression of Nde1. (a-b) Analysis of rate of differentiation of *Lis1*$^{-/-}$ cells with or without Nde1 overexpression. Equal numbers of KLS cells (Exp. #1 and Exp. #2) or KLS CD48^{-} CD150^{+} (Exp. #3) isolated from *Lis1*$^{f/f}$*; Rosa-creER* mice and infected with Nde1 or Vector were treated with 4-OH tamoxifen *in vitro*. Representative FACS plot showing data from Exp. #1 **(a)**, and frequency of cells expressing lineage markers in *Lis1*$^{-/-}$ (+Vector) and *Lis1*$^{-/-}$ (+Nde1) populations 24 hours post-deletion **(b)** individually plotted for each experiment.

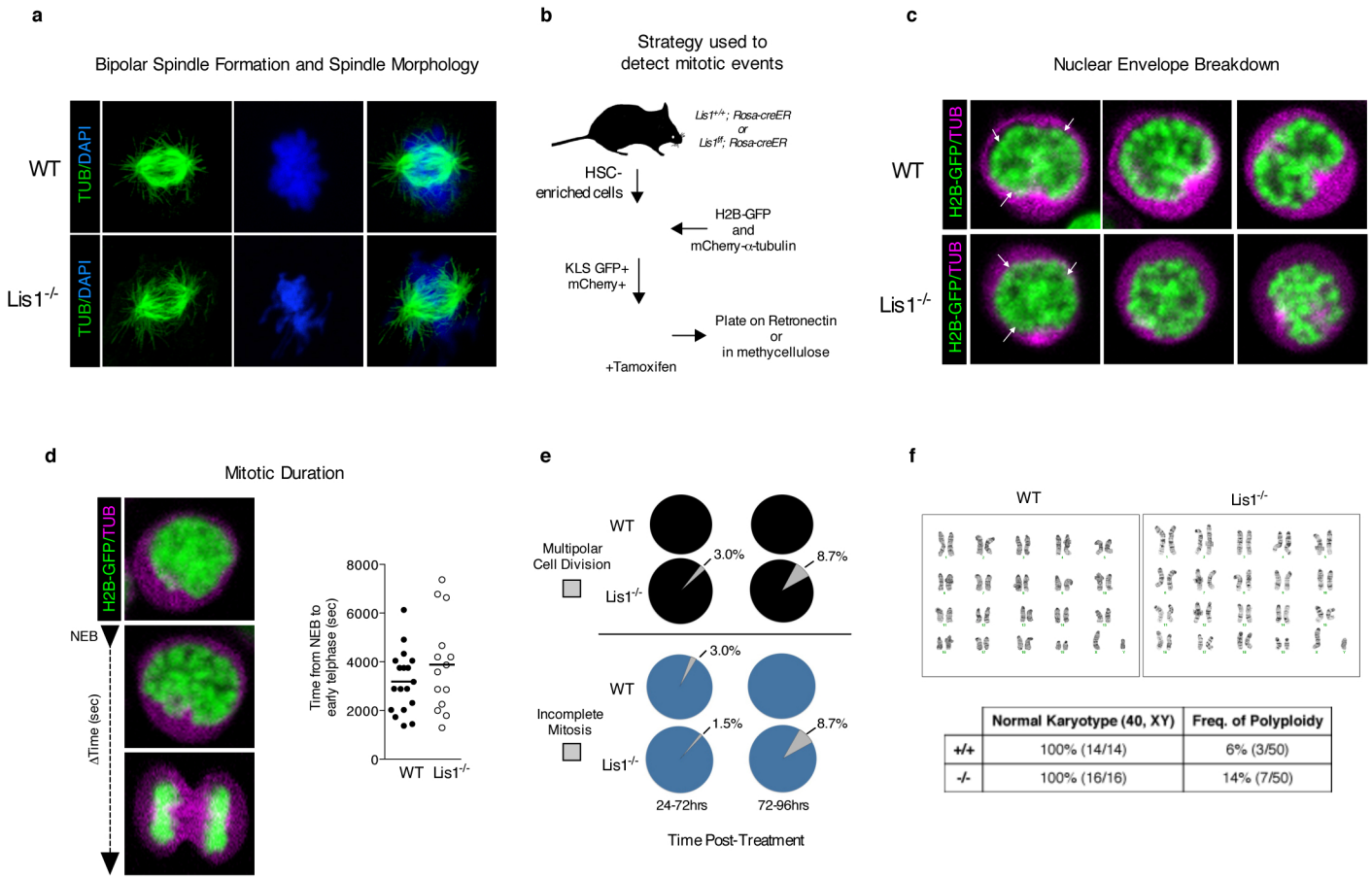

	Normal Karyotype (40, XY)	Freq. of Polyploidy
+/+	100% (14/14)	6% (3/50)
-/-	100% (16/16)	14% (7/50)

Supplementary Figure 15. Analysis of mitotic events in the *Lis1*-deficient cells.
(a) Bipolar spindle formation and spindle morphology of *Lis1*$^{-/-}$ HSCs (KLS CD48^{-}). Representative images of control (WT) and *Lis1*$^{-/-}$ cells immunostained for anti-α-tubulin antibody (green) and DAPI (blue). **(b)** Schematic illustrates the strategy used to visualize cell division in real-time. **(c)** Representative images of a control (WT) and *Lis1*$^{-/-}$ cell undergoing nuclear envelope breakdown (NEB)/chromosome condensation. H2B (green), α-tubulin (magenta). White arrows indicate NEB; *n*=18 cells for WT and *n*=14 cells for *Lis1*$^{-/-}$. **(d)** Duration of mitosis of *Lis1*$^{-/-}$ cells. Representative images of a *Lis1*$^{-/-}$ cell at the onset of NEB and at early telophase. Graph on right shows quantification of duration of mitosis; *n*=18 tracked control (WT) cells and *n*=14 tracked *Lis1*$^{-/-}$ cells. **(e)** Percentage of control (WT) and *Lis1*$^{-/-}$ cells that underwent a multipolar cell division or an incomplete mitosis. (*n*=67 cells per genotype tracked between 24-72 hrs and *n*=23 cells per genotype tracked between 72-96 hrs). **(f)** Karyotype of *Lis1*$^{-/-}$ cells. Representative G-banded karyogram of a control (WT) and *Lis1*$^{-/-}$ cell (top) and table showing the percent of control (+/+) and *Lis1*$^{-/-}$ (-/-) cells with normal karyotypes and the frequency of polyploidy (bottom).

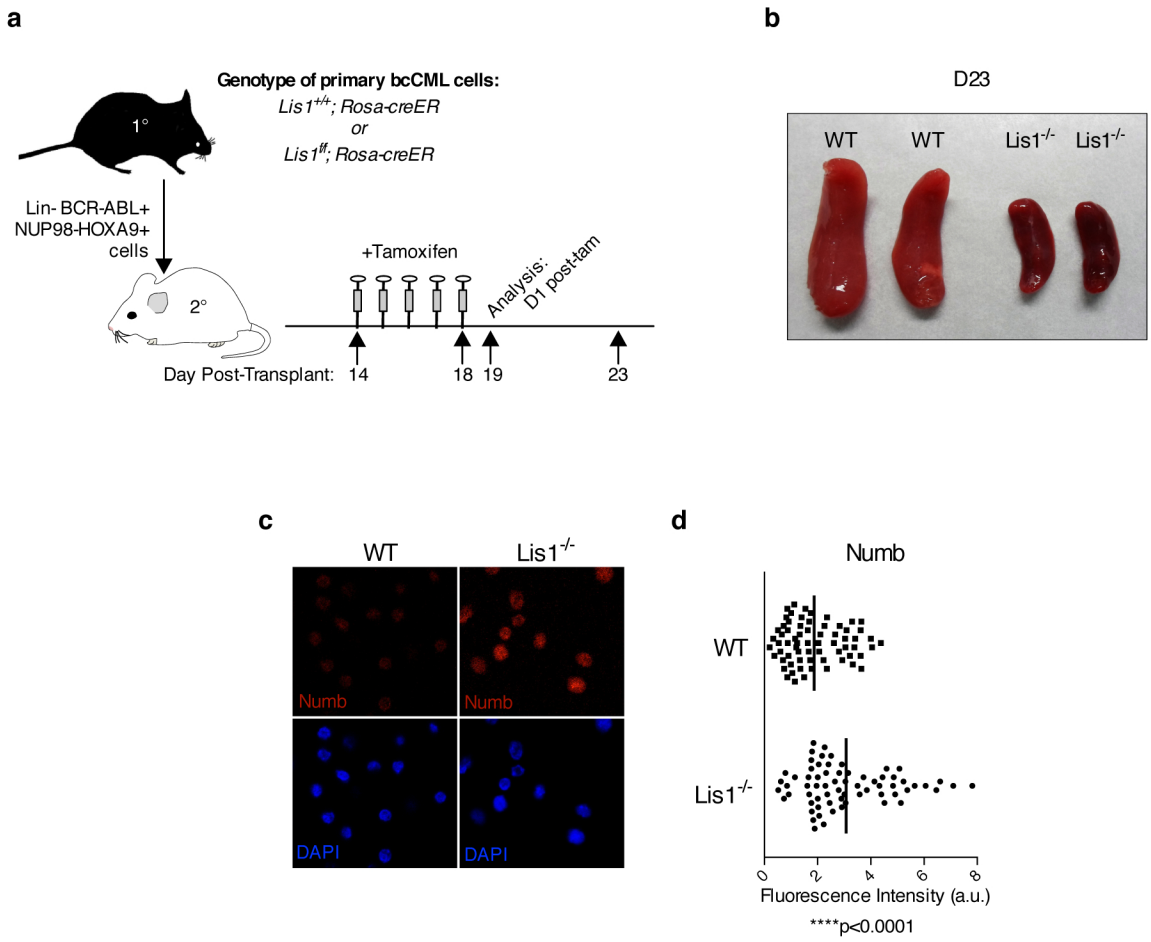

Supplementary Figure 16. Deletion of *Lis1* leads to resolution of bcCML disease and a rise in Numb levels.

Experimental scheme to track the growth and cellular behavior of bcCML *in vivo*. 40,000 lineage-negative (Lin^-) cells from control *Lis1*$^{+/+}$*; Rosa-creER* or *Lis1*$^{f/f}$*; Rosa-creER* established bcCML were transplanted into secondary recipients and two-weeks post-transplantation (on D14), tamoxifen was administered for 5 consecutive days (D14-D18). **(b)** Representative image shows control (WT) and *Lis1*$^{-/-}$ spleens 5 days post-tamoxifen treatment (on D23). **(c)** Representative image shows control (WT) and *Lis1*$^{-/-}$ leukemia cells stained with anti-Numb antibody (red) and DAPI (blue), 63X. **(d)** Average fluorescence intensity of Numb in individual bcCML cells (n=67 cells each, ***P<0.0001).

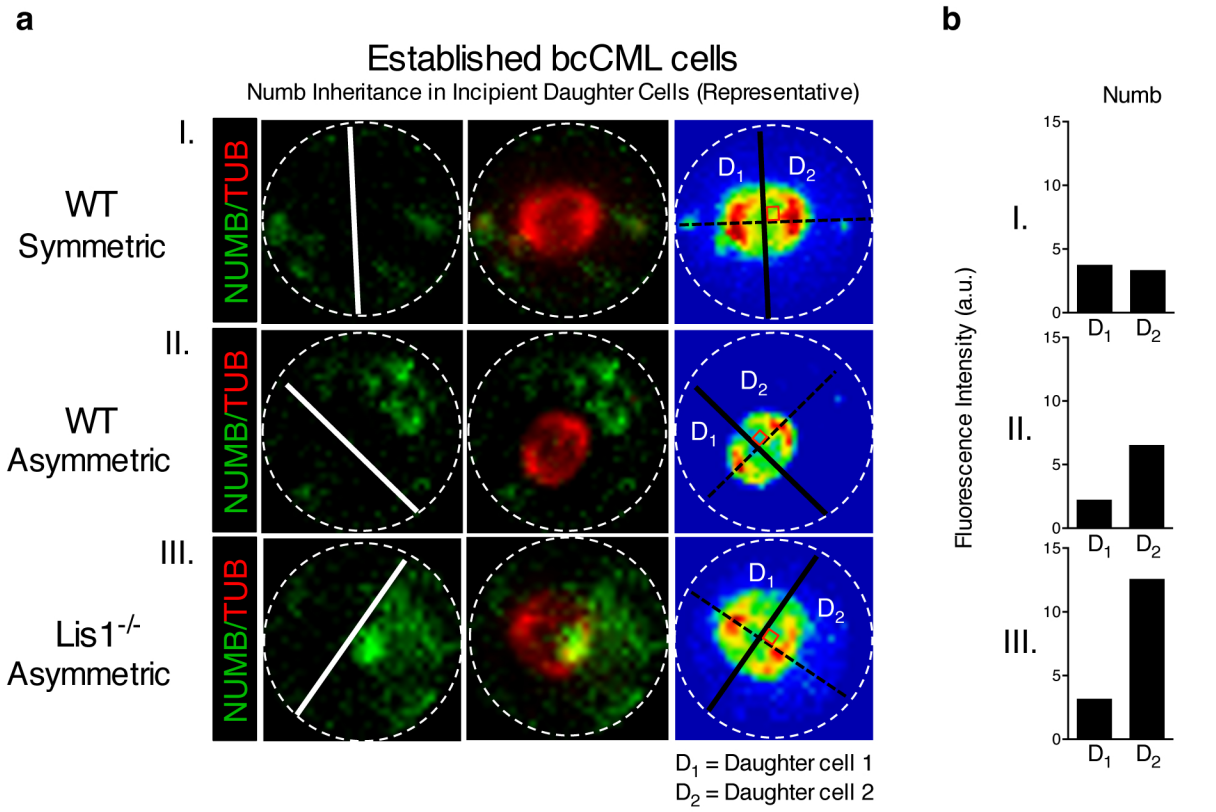

Supplementary Figure 17. Dividing leukemia cells predominantly inherit Numb asymmetrically in the absence of Lis1. (a) Numb distribution in dividing leukemia cells relative to mitotic spindle orientation. Representative images of control (WT) established blast crisis CML (bcCML) cells (I and II) or *Lis1*$^{-/-}$ established bcCML cells (III) with examples of symmetric (I) or asymmetric (II, III) inheritance of Numb by incipient daughter cells. Numb (green), α-tubulin (red). On far right panel, each cell is displayed in spectrum color format to facilitate accurate identification of spindle position (dotted black line connecting the two centrosomes highlighted in red) and the cleavage furrow (solid lines; white and black) which partitions the dividing leukemia cell into incipient daughter 1 (D_1) and daughter 2 (D_2). **(b)** Quantification of fluorescence intensity of Numb in D_1 and D_2 for each representative control (WT; I and II) or *Lis1*$^{-/-}$ cell (III) shown in **(a)**.

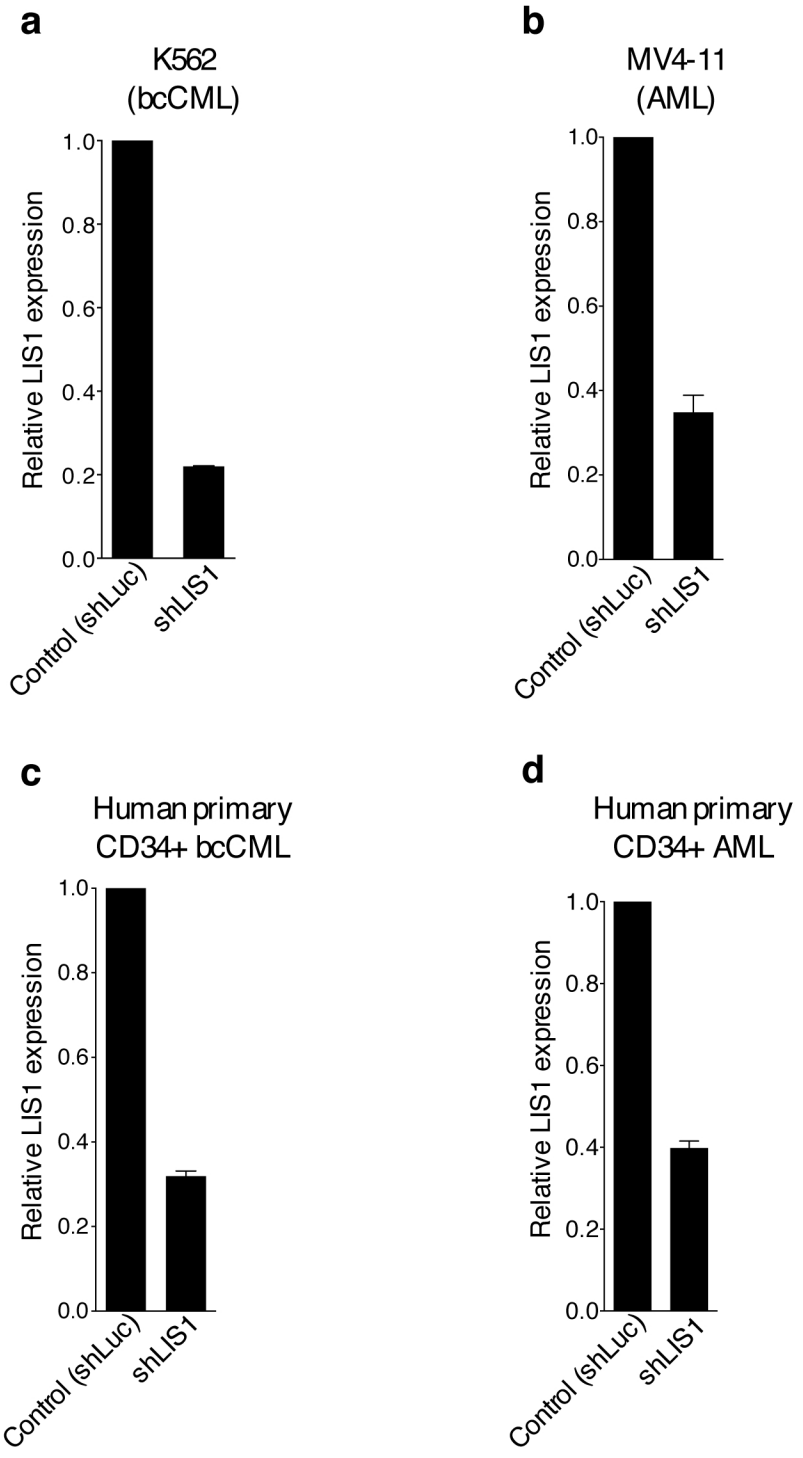

Supplementary Figure 18. Efficiency of shRNA knockdown of *LIS1* in human leukemia. **(a-d)** Realtime RT-PCR analysis of *LIS1* mRNA expression in **(a)** K562 blast crisis CML cells, **(b)** MV4-11 AML cells, **(c)** human primary $CD34^+$ bcCML, and **(d)** human primary $CD34^+$ AML following transduction with either firefly luciferase shRNA as a control (shLuc) or *LIS1* shRNA (shLIS1). Expression levels were normalized to beta-2-microglobulin and displayed relative to the control arbitrarily set at 1. Error bars represent standard error of the mean (SEM) of triplicate PCRs.

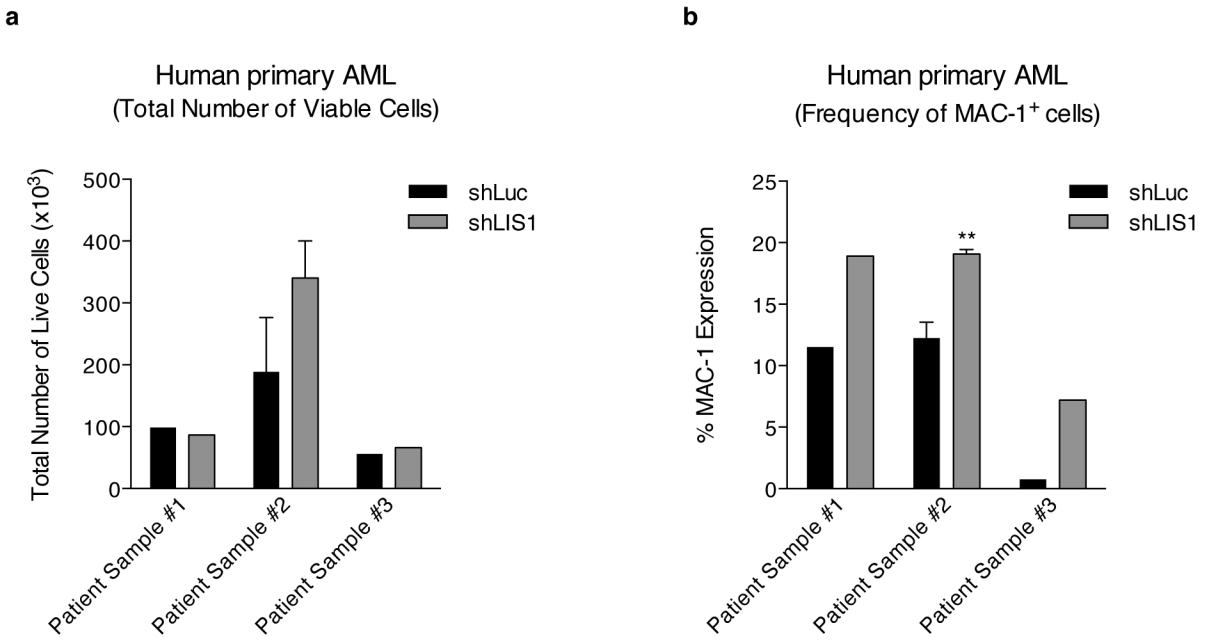

Supplementary Figure 19. Inhibition of LIS1 in primary human patient AML samples leads to accelerated differentiation. Mononuclear cells from three primary human AML samples (Patient Sample #1, #2, and #3) were infected with either control (shLuc) or lentiviral shRNA targeting human *LIS1* (shLIS1). Cell numbers were determined **(a)** and infected cells were analyzed for MAC-1 expression **(b)** at 72 hrs post-infection (Patient Samples #1 and #2) or 24 hrs post-infection (Patient Sample #3). ***P*=0.0071 for Patient Sample #2, the only sample from which a sufficient number of cells was obtained to plate in triplicate.

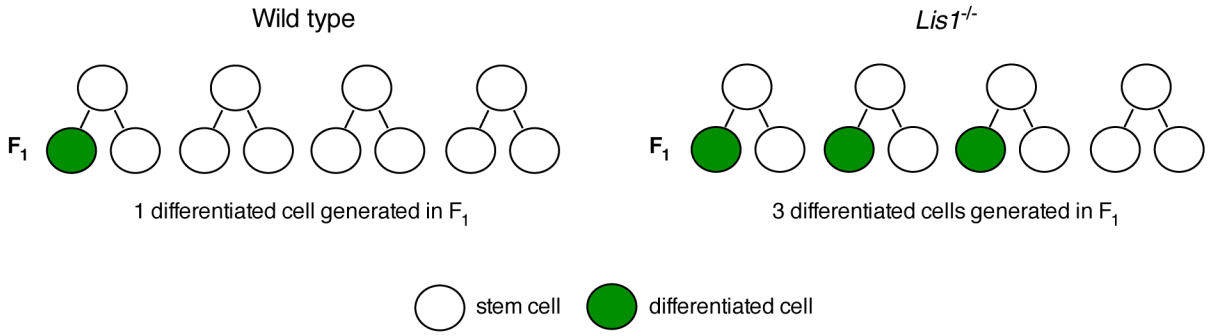

Supplementary Figure 20. Model showing how an increase in asymmetric division could generate more differentiated cells over time. Lis1 loss leads to increased asymmetric division. An increase in asymmetric division would be expected to generate more differentiated cells (green circles) at the expense of stem cells (white circles) over time.

Stage	Genotype				p-value
	Lis1$^{f/+}$	*Lis1*$^{f/f}$	*Lis1*$^{f/+}$; *Vav-Cre*	*Lis1*$^{f/f}$; *Vav-Cre*	
12.5 dpc	25	28	18	19	0.38
14.5 dpc	8	9	5	11	0.52
15.5 dpc	3	2	0	2	0.44
18.5 dpc	9	7	8	0	*0.04
Postnatal	140	94	110	0	***2.02x10^{-27}

Supplementary Table 1. Genotype of offspring derived from the cross of *Lis1*$^{f/f}$ and *Lis1*$^{f/+}$; *Vav-Cre* mice. Chi-square test was used to determine deviation from Mendelian ratios.

Primer Name	Primer Sequence
Lis1-Common-R	5′-GCTTGTTCATCAAGCTTGCAC-3′
Lis1-F_VI	5′-GCTTCCTGTTCA GCAGATATG-3′
Lis1-F_II	5′-GGCGATGATAACCACTGAGTC-3′
Lis1-F	5′-TGGATTCCCCGTCCACCTGA-3′
Lis1-R	5′-TTGGCCGCACCATACGTACC-3′
GAPDH-F	5′-CAATGACCCCTTCATTGACC-3′
GAPDH-R	5′-TTGATTTTGGAGGGATCTCG-3′
Numb-F	5′-ATGAGTTGCCTTCCACTATGCAG-3′
Numb-R	5′-TGCTGAAGGCACTGGTGATCTGG-3′
Tbp-F	5′-GTATCTACCGTGAATCTTGGCTG-3′
Tbp-R	5′-AGTTGTCCGTGGCTCTCTTATTC-3′
B2m-F	5′-ACCGGCCTGTATGCTATCCAGAA-3′
B2m-R	5′-AATGTGAGGCGGGTGGAACTGT-3′
LIS1-F	5′-CATGAGCATGTGGTAGAATGC-3′
LIS1-R	5′-GGCCCAGGTTTACCACTTTT-3′
B2M-F	5′-ATGAGTATGCCTGCCGTGTGA-3′
B2M-R	5′-GGCATCTTCAAACCTCCATG-3′

Supplementary Table 2. Primer sequences for genotyping and RT-PCR.

Supplementary Video 1. Imaging Cell Division in Real Time.

Cells were co-infected with H2B-GFP and mCherry-α-tubulin fusion constructs and imaged over time. Representative movies show A. HeLa cell, B. M1 cell, and C. Primary Hematopoietic Stem & Progenitor cells undergoing cell division (H2B-GFP is shown in green and α-tubulin is shown in magenta).

Supplementary Video 2. Symmetric inheritance of Numb.

HSC-enriched cells (KLS) were co-infected with Numb-CFP and mCherry-α-tubulin fusion constructs and imaged over time. Representative movie shows a KLS cell undergoing symmetric division (Numb is shown in green and α-tubulin is shown in red).

Supplementary Video 3. Asymmetric inheritance of Numb.

HSC-enriched cells (KLS) were co-infected with Numb-CFP and mCherry-α-tubulin fusion constructs and imaged over time. Representative movie shows a KLS cell undergoing asymmetric division (Numb is shown in green and α-tubulin is shown in red).

Supplementary Video 4. Asymmetric inheritance of Numb.

HSC-enriched cells (KLS) were co-infected with Numb-YFP and mCherry-α-tubulin fusion constructs and imaged over time. Representative movie shows a KLS cell undergoing asymmetric division (Numb is shown in green and α-tubulin is shown in red).

References for Supplementary Data

1 Wong, D. J. *et al*. Module map of stem cell genes guides creation of epithelial cancer stem cells. *Cell Stem Cell* **2**, 333-344 (2008).

2 Venezia, T. A. *et al*. Molecular signatures of proliferation and quiescence in hematopoietic stem cells. *PLoS Biol* **2**, e301 (2004).

3 Eppert, K. *et al*. Stem cell gene expression programs influence clinical outcome in human leukemia. *Nat Med* **17**, 1086-1093 (2011).